

# lncRNA MIAT promotes cell invasion and migration in esophageal cancer

WEIGUO ZHANG, QIANG CHEN and CAIPENG LEI

Department of Surgical Oncology, First Affiliated Hospital of Henan University of Science and Technology, Luoyang, Henan 471003, P.R. China

Received July 31, 2018; Accepted February 22, 2019

DOI: 10.3892/etm.2020.8588

**Abstract.** Long non-coding RNAs (lncRNAs) serve crucial roles in carcinogenesis. Myocardial infarction-associated transcript (MIAT), originally isolated as a candidate gene for myocardial infarction, has been revealed to serve as an oncogene in chronic lymphocytic leukaemias and neuroendocrine prostate cancer. However, little is known about its expression pattern, biological function and underlying mechanism in esophageal cancer. Cell lines of esophageal cancer were used in the current study. The results of the present study revealed that MIAT knockdown decreased cell viability, migration, invasion and cell cycle arrest in the G1 phase. Mechanistic assessment revealed that MIAT interacts with histone methyltransferase mixed-lineage leukemia (MLL). The relative proteins expressions were measured by western blotting assay. MIAT knockdown suppressed cell invasion and migration by regulation MMP-2/9 protein expressions. The results of the current study indicated that MIAT expression was associated with esophageal cancer and may serve as a critical target in the progression and metastasis in esophageal cancer.

## Introduction

Esophageal cancer is one of the most common malignant tumors with 400,156 deaths worldwide in 2012 and it exhibits a high incidence in China (1). Of those patients with esophageal cancer, ~90% patients are diagnosed with esophageal squamous cell carcinoma (ESCC) (1). However, a lack of progress in chemotherapy and radiotherapy has resulted in little improvement of ESCC treatment, leading to a 5-year survival rate of 15-25% (2). Previous research has primarily focused on

the role of protein encoded genes in the development of cancer and have not sufficiently assessed the effect of long non-coding RNA (lncRNA). A recent study has revealed that lncRNA may serve important biological roles in the formation, progression, invasion and metastasis of various tumors (3). lncRNAs also serve important roles in oncogenes and tumor suppressor genes by regulating their target genes or signaling pathways (4). H19 was the first tumor-associated lncRNA identified (5). It is abnormally expressed in many different types of cancer, including gastric, colon, liver and breast cancer and is involved in the regulation of tumor cell proliferation, apoptosis, invasion and migration (6,7). MEG3 is the first lncRNA that has been determined to inhibit tumor function (8). MEG3 inhibits proliferation and promotes cell apoptosis by regulating the expression of p53 (9). A previous study reported that when the lncRNA myocardial infarction-associated transcript (MIAT) is knocked-out in mice, they do not exhibit any significant abnormality with cancer development, but are increasingly hyperactive (10). Furthermore a previous study demonstrated that MIAT is significantly increased in cancer lesions (11). In digestive tract cancer, previous studies have determined that MIAT is highly expressed in gastric cancer (12,13), colorectal cancer (14) and hepatocellular carcinoma (15,16).

However, the function and mechanism of the majority of lncRNAs are yet to be fully elucidated. The current study assessed the viability, apoptosis, invasion and migration of MIAT in esophageal cancer cells. The results of the current study may help identify novel therapeutic targets in esophageal cancer.

## Materials and methods

**Cell culture and transfection.** HEEC, TE-1, Kyse 30, Kyse 180, Kyse 510, Kyse 150 and Eca 109 cell lines (American Type Culture Collection, Manassas, VA, USA) were respectively cultured in RPMI 1640 medium (Thermo Fisher Scientific, Inc., Waltham, MA, USA) containing 10% fetal bovine serum (FBS; Gibco; Thermo Fisher Scientific, Inc.), 100 mg/ml streptomycin and 100 U/ml penicillin. Cells were then incubated at 37°C with 5% CO<sub>2</sub>. Kyse 150 and Eca 109 cells were respectively transfected with 25 or 50 nM of small interfering (si) RNA using RNAiMAX Lipofectamine (Invitrogen; Thermo Fisher Scientific, Inc.) in accordance with the manufacturer's protocol. The lncRNA MIAT siRNA (siMIAT) sequence

---

*Correspondence to:* Dr Weiguo Zhang, Department of Surgical Oncology, First Affiliated Hospital of Henan University of Science and Technology, 24 Jinghua Road, Jianxi, Luoyang, Henan 471003, P.R. China  
E-mail: wgz\_zhang@163.com

**Key words:** long non-coding RNA, myocardial infarction-associated transcript, esophageal cancer, matrix metalloproteinase 9, Eca 109, Kyse 150

was 5'-ACUUCUUCGUAUGUUCGGCTT-3'. Kyse 150 and Eca 109 cells were divided into negative control (NC) transfected by siRNA-NC (5'-GCACCTTGAGTGAATGTCAGGGACTCCCTGATGATGTGA-3'), 25 and 50 nM groups, respectively. Samples were incubated for 24 h before subsequent experimentation.

**Reverse transcription-quantitative polymerase chain reaction (RT-qPCR) assay.** Total RNA was extracted from HEEC, TE-1, Kyse 30, Kyse 180, Kyse 510, Kyse 150 and Eca 109 cells using a TRIzol kit (Thermo Fisher Scientific, Inc.) and cDNA was subsequently synthesized using the cDNA synthesis kit (Thermo Fisher Scientific, Inc.) and qPCR was performed using the qPCR kit (Takara Bio, Inc., Otsu, Japan) to measure mRNA expression by SYBR-Green method. The following primer sequences (synthesized by Shenzhen Huada Gene Biotechnology Co., Ltd., Shenzhen, China) were utilized as following: MIAT forward, 5'-GCTCACACCTCCTATTCCT-3' and reverse, 5'-CTTCACCAACTCTCCCACT-3'. U6 (nuclear reference) forward, 5'-CTCGCTTCGGCAGCA CA-3' and reverse, 5'-AACGCTTCACGAATTTGCGT-3'; 18S (cytoplasmic reference forward, 5'-GTGGGCCGAAGATATGCTCA-3' and reverse, 5'-TTGGCTAGGACCTGGCTGTA-3'. The thermocycling conditions were as follows: 95°C for 5 min; followed by 40 cycles of 95°C for 30 sec, 60°C for 30 sec and 72°C for 30 sec.

**MTT assay.** A total of 24 h following treatment, Kyse 150 and Eca 109 cells in suspension ( $2 \times 10^5$  cells/ml) were inoculated into 96-well plates. Following culture for 48 h, 10  $\mu$ l MTT was added to each well and cultured for 4 h. The supernatant was subsequently removed and 100  $\mu$ l DMSO was added to wells to dissolve the purple formazan. Absorbance was measured at 570 nm and cell viability was determined.

**Flow cytometry.** Kyse 150 and Eca 109 cells of different groups (NC, 25 and 50 nM groups) were collected and adjusted to a concentration of  $1 \times 10^6$  cell/ml. Cells then underwent centrifugation at  $1,000 \times g$  for 5 min, following which the supernatant was discarded. Samples were then washed twice with cold PBS and centrifuged for a further 5 min at  $1,500 \times g$  at 4°C. Cells were resuspended using cooled 70% EtOH and fixed with 70% EtOH overnight at 4°C. The following day, samples were centrifuged ( $1,500 \times g$ ; 10 min; 4°C), washed once with PBS, washed twice with normal saline and centrifuged a second time ( $1,500 \times g$ ; 5 min; 4°C). Cells were then stained with Propidium iodide (50 mg/l; Triton X-100, 1.0%; RNase A, 10 mg/l; Thermo Fisher Scientific, Inc.) at 4°C in the dark for 30 min. A flow cytometer was used to measure early and late stage cell apoptosis and the cell cycle by flow cytometry (Coulter Epics Altra flow cytometer; Beckman Coulter).

**Transwell assay.** Kyse 150 and Eca 109 cells of different groups (NC, 25 and 50 nM) were cultured in 20% culture medium, trypsinised then suspended in serum-free medium (Thermo Fisher Scientific, Inc.). Cells were plated at a density of  $1 \times 10^5$  cells/well in the upper chamber with 20  $\mu$ l Matrigel. Complete medium (600  $\mu$ l; Thermo Fisher Scientific, Inc.) containing 20% FBS was added to the lower chamber. Samples were then routinely cultured for 24 h at 37°C and washed twice with PBS. Following

cell fixation with 4% polyoxymethylene at room temperature for 30 min and staining at 37°C for 2 h with crystal violet, the number of cells in 5 random fields of view were counted using an optical light microscope (ECLIPSE Ts2; Nikon Corporation) at  $\times 200$  magnification.

**Wound healing assay.** Kyse 150 and Eca 109 cells of different groups were cultured for 24 h at 37°C. Cells were then suspended in culture medium, routinely digested by protein trypsinase, (Sigma-Aldrich; Merck KGaA, Darmstadt, Germany) adjusted to a concentration of  $5 \times 10^5$  cells/well and inoculated onto 6-well plates. When cells were completely confluent, a 200  $\mu$ l pipette tip was used to create a scratch. A total of 2 ml of serum free culture medium (RPMI 1640 medium) was added at room temperature for 30 min then incubated. The distance between cells following wound induction were observed and imaged using an inverted microscope (magnification,  $\times 100$ ) at 0 and 48 h. Wound healing rate was then calculated using Image-Pro Plus software (Version X; Media Cybernetics, Silver Springs, MD, USA).

**Western blotting.** Total protein from Kyse 150 and Eca 109 cells in different groups were extracted using radioimmunoprecipitation lysis buffer (150 mM NaCl, 0.1% SDS, 0.5% sodium deoxycholate, 1% NP-40; Sigma-Aldrich; Merck KGaA). Protein concentration was also measured using the bicinchoninic acid method. Equal quantities of total protein (50  $\mu$ g) were separated on 10% SDS-PAGE gels and transferred to polyvinylidene difluoride membranes. Membranes were blocked using 1% bovine serum albumin (Beyotime Institute of Biotechnology) at room temperature for 2 h. The following primary antibodies (all 1:1,000; Abcam, Cambridge, UK) were then added to membranes and incubated overnight at 4°C: histone methyltransferase mixed-lineage leukemia (MLL; cat. no. ab32400), cyclin-dependent kinase 2 (Cdk2; cat. no. ab32147), Cyclin D3 (cat. no. ab28283), matrix metalloproteinase-2 (MMP-2; cat. no. ab37150), MMP-9 (cat. no. ab73734) and GAPDH (cat. no. ab9485). Subsequently, membranes were incubated with horseradish-peroxidase conjugated goat anti-rabbit secondary antibodies (1:5,000; Santa Cruz Biotechnology, Inc.) for 1.5 h at room temperature. Electrochemiluminescence kit (EMD Millipore, Billerica, MA, USA) was used to visualize protein signals and bands were analyzed using ImageJ v1.42 software (National Institutes of Health, Bethesda, MD, USA). GAPDH was utilized as an internal control in this experiment.

**Statistical analysis.** Statistical data were analyzed using GraphPad Prism software (version 5.0; GraphPad Software, Inc., La Jolla, CA, USA). Values are expressed as the mean  $\pm$  standard deviation from three independent experiments. The differences between two groups were analyzed using two-tailed Student's t-tests. The differences amongst more than two groups were analyzed using one-way analysis of variance followed by Tukey's post-hoc test.  $P < 0.05$  was considered to indicate a statistically significant difference.

## Results

**MIAT gene expression.** The results of RT-qPCR revealed that the expression of MIAT in esophageal cancer cell lines

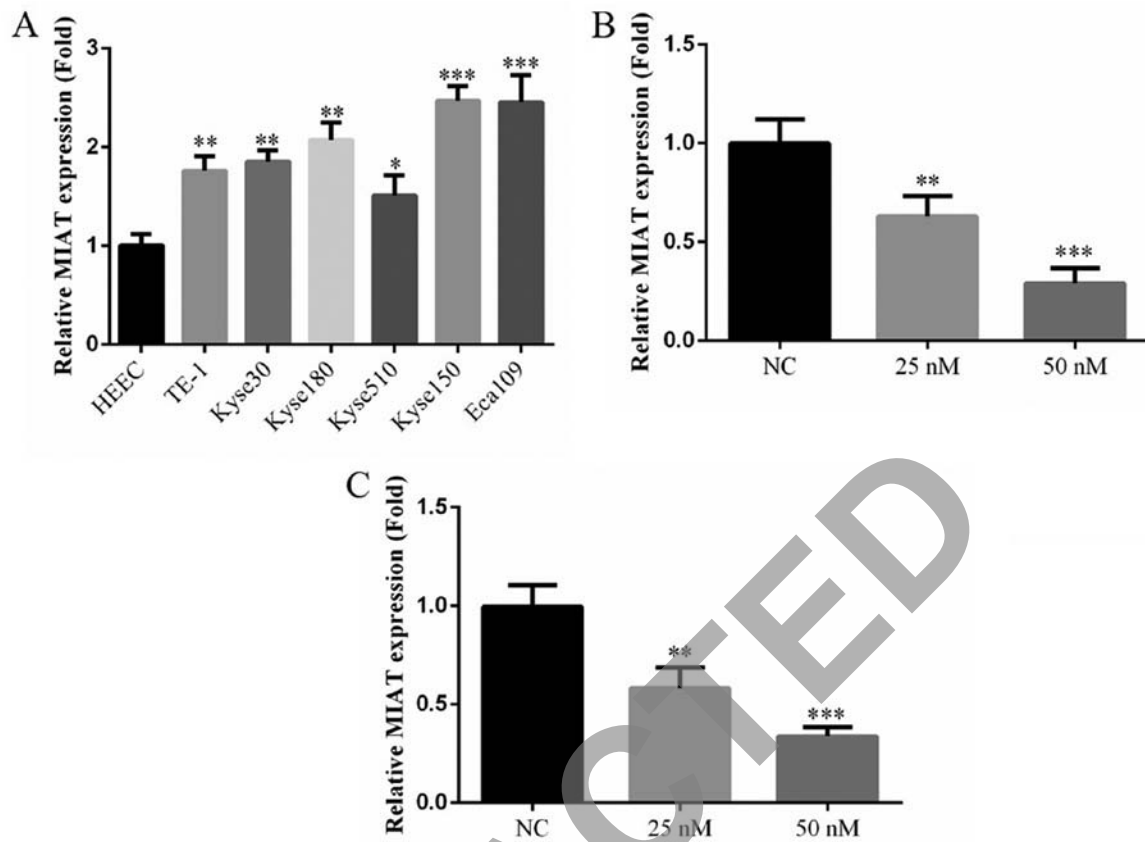


Figure 1. MIAT expression of siMIAT transfected Kyse 150 and Eca 109 cells. (A) The expression of MIAT in different cell lines, as determined via reverse-transcription-quantitative polymerase chain reaction. Cells were transfected with siMIAT (25 or 50 nM) and the expression of MIAT was subsequently determined in (B) Kyse 150 and (C) Eca 109 cells. \* $P < 0.05$ , \*\* $P < 0.01$  and \*\*\* $P < 0.001$  vs. the NC group. MIAT, myocardial infarction-associated transcript; si, small interfering RNA; NC, negative control.

were significantly increased compared with normal esophageal cells (HEEC; Fig. 1A). Furthermore, of the esophageal cancer cell lines used, the expression of MIAT was highest in Kyse 150 and Eca 109 cells. Following siMIAT transfection at 25 and 50 nM concentrations, the expression of MIAT was significantly decreased in Kyse 150 and Eca 109 cells compared with NC cells (Fig. 1B and C). MIAT expression was highest in Kyse 150 and Eca 109 cells therefore these cell lines were selected for further experimentation.

*si-MIAT affects cell viability.* As determined by the MTT assay, the growth rate of Kyse 150 and Eca 109 cells were significantly and dose-dependently decreased following siMIAT transfection compared with NC cells (Fig. 2A and B). These results indicate that MIAT enhances the viability of certain ESCC cell lines.

*MIAT knockdown improves cell apoptosis.* The results of flow cytometry demonstrated that the rate of cell apoptosis in siMIAT-treated Kyse 150 and Eca 109 cells was dose-dependent and significantly upregulated compared with NC-treated cells (Fig. 3).

*siMIAT affects the cell cycle.* To determine whether MIAT causes cell cycle arrest, the cell cycle was analyzed via flow cytometry. The results revealed that 25 and 50 nM siMIAT transfection significantly and dose-dependently

increased Kyse 150 and Eca 109 cell G1 phase compared with NC cells (Fig. 4). Transfection with 25 and 50 nM siMIAT significantly decreased Kyse 150 and Eca 109 cell G2 and S phase compared with NC cells in a dose-dependent manner.

*MIAT knockdown affects cell invasion.* To assess the efficiency of MIAT on the invasion of Kyse 150 and Eca 109 cells, a transwell assay was performed. The results revealed that transfection with siMIAT suppresses the invasion of Kyse 150 and Eca 109 cells in a dose-dependent manner when compared with NC treated cells (Fig. 5).

*MIAT silencing depresses cell invasion in the wound healing assay.* To further assess the effect of MIAT on Kyse 150 and Eca 109 cell invasion, a wound healing assay was performed. The results demonstrated that at 48 h following wound induction, siMIAT transfection significantly and dose-dependently decreased Kyse 150 and Eca 109 cell invasion compared with NC cells (Fig. 6).

*MIAT knockdown affects relative protein expression.* The results of western blotting revealed that the expression of MLL, Cdk2, Cyclin D3, MMP-2 and MMP-9 in Kyse 150 and Eca 109 cells transfected with siMIAT was significantly and dose-dependently decreased compared with NC treated cells (Fig. 7).

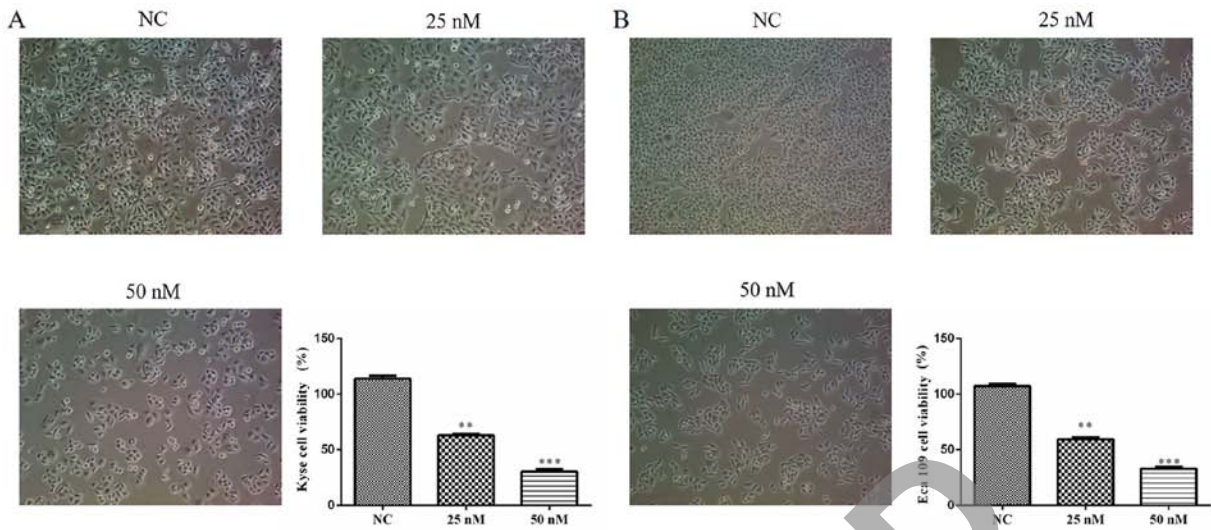


Figure 2. Viability of siMIAT transfected Kye 150 and Eca 109 cells. The viability of (A) Kye 150 and (B) Eca 190 cells was determined following (25 or 50 nM) siMIAT transfection via an MTT assay. \*\* $P < 0.01$  and \*\*\* $P < 0.001$  vs. the NC group. NC, negative control.

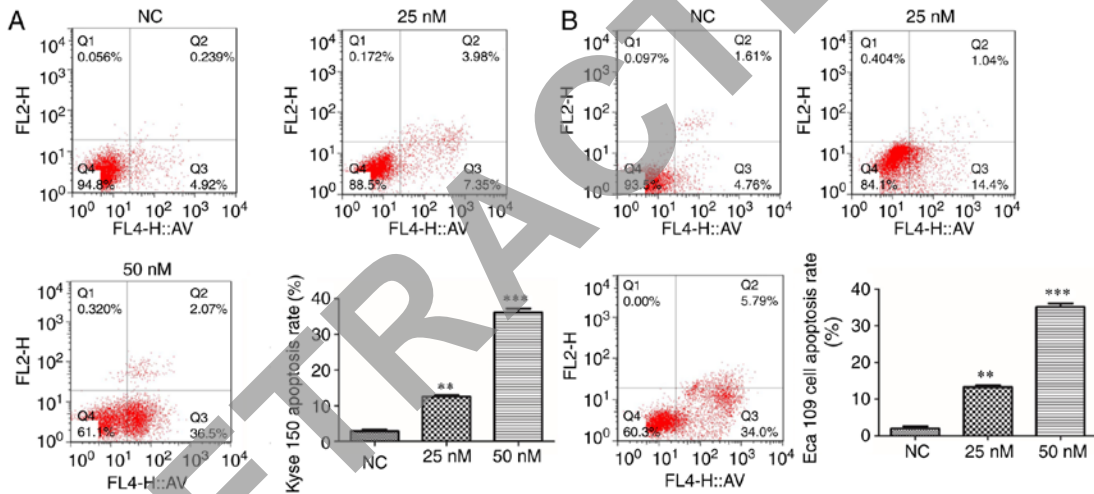


Figure 3. Apoptosis of siMIAT transfected Kye 150 and Eca 109 cells. The apoptosis of (A) Kye 150 and (B) Eca 109 cells transfected with (25 or 50 nM) siMIAT was determined via flow cytometry. \*\* $P < 0.01$  and \*\*\* $P < 0.001$  vs. the NC group. siMIAT, small interfering RNA myocardial infarction-associated transcript; NC, negative control; FL4H:AV, wavelength 640-680 nm.

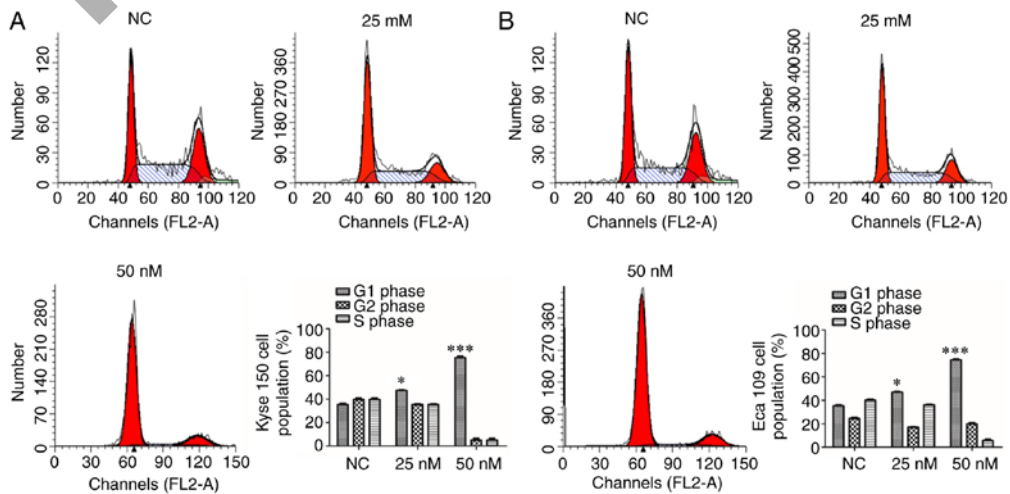


Figure 4. Cell cycle analysis of siMIAT transfected Kye 150 and Eca 109 cells. The cell cycles of (A) Kye 150 and (B) Eca 109 cells transfected with 25 or 50 nM siMIAT were determined via flow cytometry. \* $P < 0.05$  and \*\*\* $P < 0.001$  vs. the NC group. siMIAT, small interfering RNA myocardial infarction-associated transcript; NC, negative control; FL2-A, Pulse area.

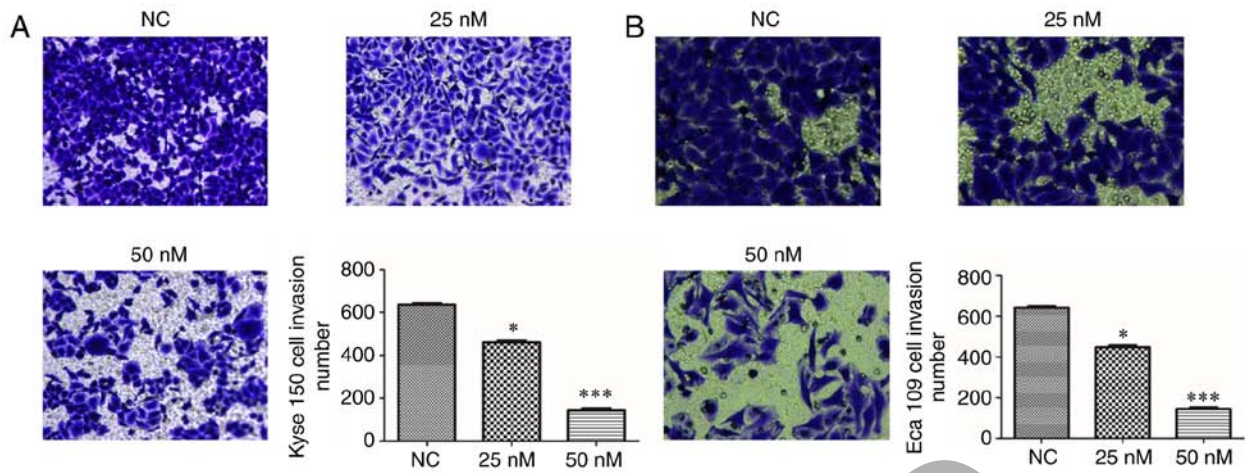


Figure 5. Invasion of siMIAT transfected Kyse 150 and Eca 109 cells. (A) The invasion of (A) Kyse 150 and (B) Eca 109 cells transfected with 25 or 50 nM siMIAT was determined via a Transwell assay. \*P<0.05 and \*\*\*P<0.001 vs. the NC group. siMIAT, small interfering RNA myocardial infarction-associated transcript; NC, negative control.

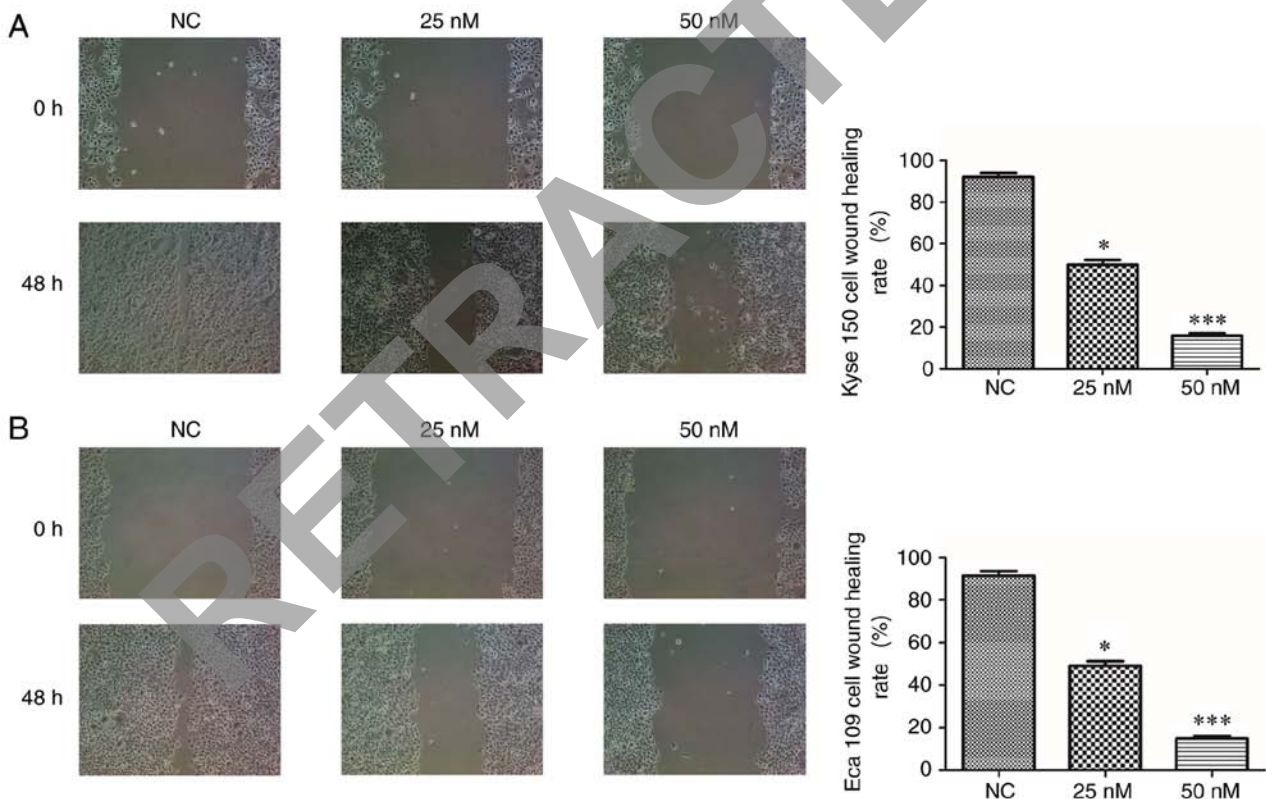


Figure 6. Wound healing rate of siMIAT transfected Kyse 150 and Eca 109 cells. The wound healing rate of (A) Kyse 150 and (B) Eca 109 cells transfected with 25 or 50 nM siMIAT was determined via a wound healing assay. \*P<0.05 and \*\*\*P<0.001 vs. the NC group. siMIAT, small interfering RNA myocardial infarction-associated transcript. NC, negative control.

## Discussion

It is well known that lncRNA is abnormally expressed in many types of cancer and participates in the regulation of tumor development. It is therefore serves as a potential tumor marker and therapeutic target. For example, HOX Transcript Antisense RNA is highly expressed in breast, gastric and liver cancer, and increases the proliferation and invasion of tumor cells (17). Plasmacytoma variant translocation 1 is also highly

expressed in colorectal cancer and functions to regulate the invasion and metastasis of tumor cells via the transforming growth factor- $\beta$  signaling pathway (18). MIAT is a lncRNA that is located on the long arm of chromosome 22 (19). Recent studies have revealed that MIAT serves an important role in the development of a variety of diseases (20,21). However, the effects and mechanism of MIAT in esophageal cancer are yet to be fully elucidated. The results of the current study revealed that the viability, migration and invasion of two

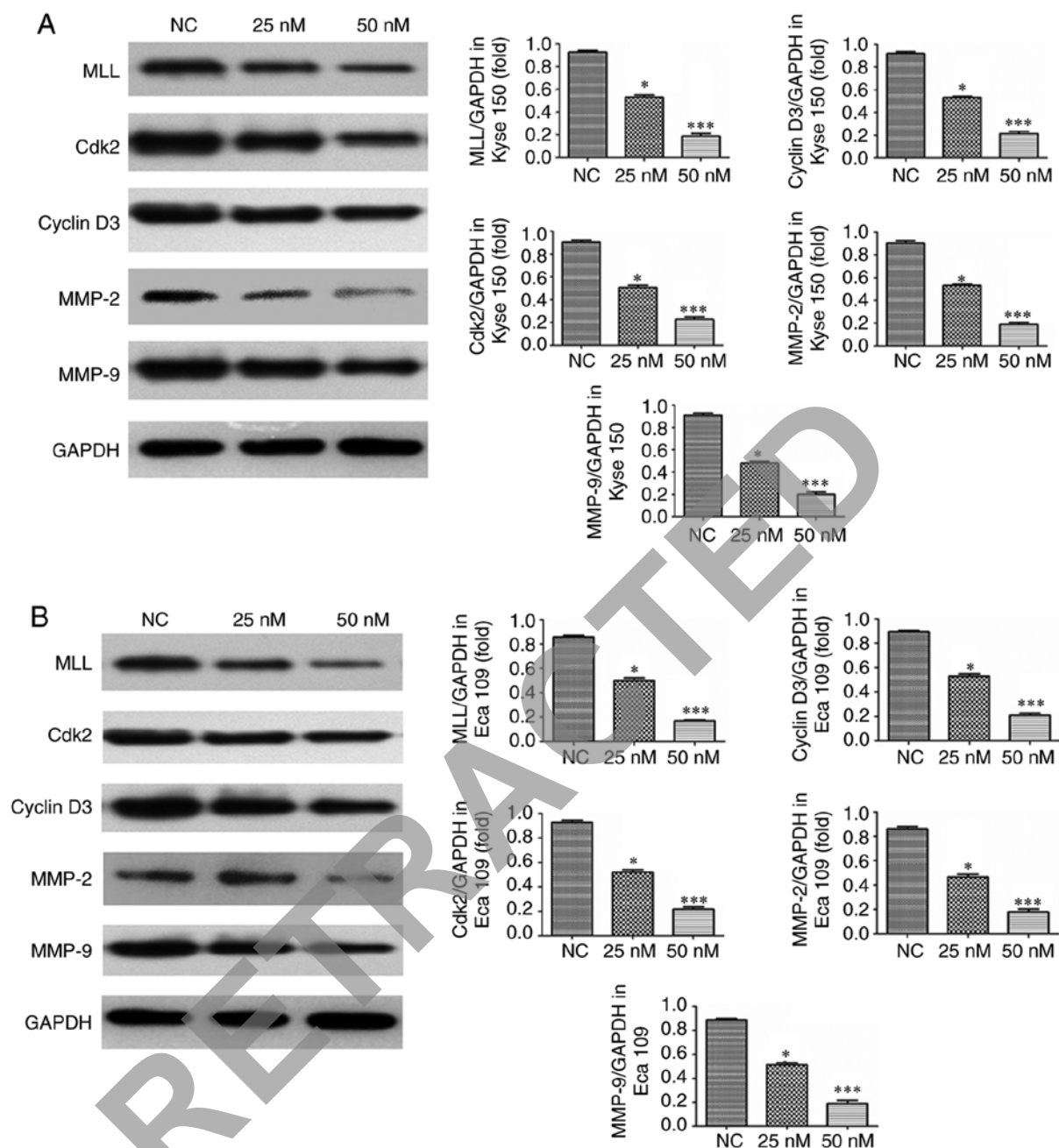


Figure 7. Relative protein expression in siMIAT transfected Kyse 150 and Eca 109 cells. The protein expression of MLL, Cdk2, cyclin D3, MMP-2 and MMP-9 in (A) Kyse 150 and (B) Eca 109 cells was determined via western blotting. \* $P < 0.05$  and \*\*\* $P < 0.001$  vs. the NC group. siMIAT, small interfering RNA myocardial infarction-associated transcript; MLL, histone methyltransferase mixed-lineage leukemia; Cdk2, cyclin-dependent kinase 2; MMP, matrix metalloproteinase; NC, negative control.

ESCC cell lines (Kyse 150 and Eca 109 cells) were significantly and dose-dependently suppressed following treatment with a si-MIAT. Future work will investigate the underlying mechanism by measuring MIAT relative protein expression.

A previous study has revealed that MIAT regulates the expression of the MLL protein in lung cancer (11). Previous studies have also demonstrated that the activation of MLL enhances cancer cell invasion and migration by regulating various MMPs (22,23). MMP overexpression closely correlates with cancer cell invasion and migration (24,25). MMP-2 and MMP-9 are two important members of the MMP family, which effectively breaks down the main components of the basement membrane (26,27). The overexpression of MMP-2

and MMP-9 may also promote cancer cell invasion and migration (28,29). Furthermore, it has been revealed that MMP-2 and MMP-9 were overexpressed in esophageal cancer (30,31). The results of the present study revealed that transfection with siMIAT suppressed the invasion and migration of Kyse 150 and Eca 109 cells dose-dependently. The underlying mechanism of MIAT attenuating esophageal cancer invasion and migration might be correlated with a reduction in MMP-2 and MMP-9 protein expression.

Cell proliferation is a process that is highly regulated and controlled by many factors including cyclin, cyclin dependent protein kinases (CDK), cyclin dependent suppressor protein (CKI). Different cells exhibit different proliferative phases,

which primarily involve the G1 phase of the cell cycle. Once a cell surpasses the restriction point of the G1 phase, the cell cycle may continue such that mitosis is achieved. Therefore, the regulation of the G1/S phase checkpoint, which involves various proteins including cyclin D1, cyclin D3, cyclin E, Cdk 2, Cdk 4 and Cdk 6 is important (32-35). The results of the current study revealed that the expression of cyclin D3 and Cdk 2 were significantly and dose-dependently decreased following siMIAT transfection. MIAT knockdown might suppress esophageal cancer cell proliferation by keeping the cell cycle in G1 phase. There were some limitations to the present study, for example the effects and mechanism of MIAT knockdown was only investigated *in vitro* therefore, future study will involve *in vivo* work.

In conclusion, MIAT knockdown suppresses esophageal cancer cell viability by enhancing the invasion, migration and G1 phase of the cell cycle *in vitro* and in future esophageal cancer treatment, MIAT might be used as a potential target gene.

#### Acknowledgements

Not applicable.

#### Funding

No funding was received.

#### Availability of data and materials

All data generated or analyzed during this study are included in this published article.

#### Authors' contributions

WZ and QC were responsible for performing the experiments, collecting the data, conducting the data analysis and interpreting the results. CL designed the experiments and wrote the manuscript. All authors read and approved the final manuscript.

#### Ethics approval and consent to participate

Not applicable.

#### Patient consent for publication

Not applicable.

#### Competing interests

The authors declare that they have no competing interests.

#### References

- Guo LW, Huang HY, Shi JF, Lv LH, Bai YN, Mao AY, Liao XZ, Liu GX, Ren JS, Sun XJ, *et al*: Medical expenditure for esophageal cancer in China: A 10-year multicenter retrospective survey (2002-2011). *Chin J Cancer* 36: 73, 2017.
- Chen W, Zheng R, Baade PD, Zhang S, Zeng H, Bray F, Jemal A, Yu XQ and He J: Cancer statistics in China, 2015. *CA Cancer J Clin* 66: 115-132, 2016.
- Jiang C, Li X, Zhao H and Liu H: Long non-coding RNAs: Potential new biomarkers for predicting tumor and metastasis. *Mol Cancer* 15: 62, 2016.
- Seles M, Hutterer GC, Kiesslich T, Pummer K, Berindan-Neagoe I, Perakis S, Schwarzenbacher D, Stotz M, Gerger A and Pichler M: Current insights into long non-coding RNAs in renal cell carcinoma. *Int J Mol Sci* 17: 573, 2016.
- Feil R, Walter J, Allen ND and Reik W: Developmental control of allelic methylation in the imprinted mouse *Igf2* and *H19* genes. *Development* 120: 2933-2943, 1994.
- Raveh E, Matouk IJ, Gilon M and Hochberg A: The H19 long non-coding RNA in cancer initiation, progression and metastasis—a proposed unifying theory. *Mol Cancer* 14: 184, 2015.
- Yang F, Bi J, Xue X, Zheng L, Zhi K, Hua J and Fang G: Up-regulated long non-coding RNA H19 contributes to proliferation of gastric cancer cells. *FEBS J* 279: 3159-3165, 2012.
- Zhang X, Zhou Y, Mehta KR, Danila DC, Scolavino S, Johnson SR and Klibanski A: A pituitary-derived MEG3 isoform functions as a growth suppressor in tumor cells. *J Clin Endocrinol Metab* 88: 5119-5126, 2003.
- Zhou Y, Zhang X and Klibanski A: MEG3 noncoding RNA: A tumor suppressor. *J Mol Endocrinol* 48: R45-R53, 2012.
- Ip JY, Sone M, Nashiki C, Pan Q, Kitaichi K, Yanaka K, Abe T, Takao K, Miyakawa T, Blencowe BJ and Nakagawa S: Gomafu lncRNA knockout mice exhibit mild hyperactivity with enhanced responsiveness to the psychostimulant methamphetamine. *Sci Rep* 6: 27204, 2016.
- Lai IL, Yang CA, Lin PC, Chan WL, Lee YT, Yen JC, Chang YS and Chang JG: Long noncoding RNA MIAT promotes non-small cell lung cancer proliferation and metastasis through MMP9 activation. *Oncotarget* 8: 98148-98162, 2017.
- Sha M, Lin M, Wang J, Ye J, Xu J, Xu N and Huang J: Long non-coding RNA MIAT promotes gastric cancer growth and metastasis through regulation of miR-141/DDX5 pathway. *J Exp Clin Cancer Res* 37: 58, 2018.
- Li Y, Wang K, Wei Y, Yao Q, Zhang Q, Qu H and Zhu G: lncRNA-MIAT regulates cell biological behaviors in gastric cancer through a mechanism involving the miR-29a-3p/HDAC4 axis. *Oncol Rep* 38: 3465-3472, 2017.
- Liu Z, Wang H, Cai H, Hong Y, Li Y, Su D and Fan Z: Long non-coding RNA MIAT promotes growth and metastasis of colorectal cancer cells through regulation of miR-132/Derlin-1 pathway. *Cancer Cell Int* 18: 59, 2018.
- Xiang Y, Huang Y, Sun H, Pan Y, Wu M and Zhang J: Deregulation of miR-520d-3p promotes hepatocellular carcinoma development via lncRNA MIAT regulation and EPHA2 signaling activation. *Biomed Pharmacother* 109: 1630-1639, 2019.
- Huang X, Gao Y, Qin J and Lu S: lncRNA MIAT promotes proliferation and invasion of HCC cells via sponging miR-214. *Am J Physiol Gastrointest Liver Physiol* 314: G559-G565, 2018.
- Rinn JL, Kertesz M, Wang JK, Squazzo SL, Xu X, Bruggmann SA, Goodnough LH, Helms JA, Farnham PJ, Segal E and Chang HY: Functional demarcation of active and silent chromatin domains in human HOX loci by noncoding RNAs. *Cell* 129: 1311-1323, 2007.
- Takahashi Y, Sawada G, Kurashige J, Uchi R, Matsumura T, Ueo H, Takano Y, Eguchi H, Sudo T, Sugimachi K, *et al*: Amplification of PVT-1 is involved in poor prognosis via apoptosis inhibition in colorectal cancers. *Br J Cancer* 110: 164-171, 2014.
- Ishii N, Ozaki K, Sato H, Mizuno H, Saito S, Takahashi A, Miyamoto Y, Ikegawa S, Kamatani N, Hori M, *et al*: Identification of a novel non-coding RNA, MIAT, that confers risk of myocardial infarction. *J Hum Genet* 51: 1087-1099, 2006.
- Zhou L, Xu DY, Sha WG, Shen L, Lu GY and Yin X: Long non-coding MIAT mediates high glucose-induced renal tubular epithelial injury. *Biochem Biophys Res Commun* 468: 726-732, 2015.
- Shen Y, Dong LF, Zhou RM, Yao J, Song YC, Yang H, Jiang Q and Yan B: Role of long non-coding RNA MIAT in proliferation, apoptosis and migration of lens epithelial cells: A clinical and in vitro study. *J Cell Mol Med* 20: 537-548, 2016.
- Takeda S, Liu H, Sasagawa S, Dong Y, Trainor PA, Cheng EH and Hsieh JJ: HGF-MET signals via the MLL-ETS2 complex in hepatocellular carcinoma. *J Clin Invest* 123: 3154-3165, 2013.

23. Robert I, Aussems M, Keutgens A, Zhang X, Hennuy B, Viatour P, Vanstraelen G, Merville MP, Chapelle JP, de Leval L, *et al*: Matrix Metalloproteinase-9 gene induction by a truncated oncogenic NF-kappaB2 protein involves the recruitment of MLL1 and MLL2 H3K4 histone methyltransferase complexes. *Oncogene* 28: 1626-1638, 2009.
24. Almeida-Rios D, Graça I, Vieira FQ, Ramalho-Carvalho J, Pereira-Silva E, Martins AT, Oliveira J, Gonçalves CS, Costa BM, Henrique R and Jerónimo C: Histone methyltransferase PRMT6 plays an oncogenic role of in prostate cancer. *Oncotarget* 7: 53018-53028, 2016.
25. Shay G, Lynch CC and Fingleton B: Moving targets: Emerging roles for MMPs in cancer progression and metastasis. *Matrix Biol* 44-46: 200-206, 2015.
26. Wang X and Khalil RA: Matrix metalloproteinases, vascular remodeling, and vascular disease. *Adv Pharmacol* 81: 241-330, 2018.
27. Wang G, Yin L, Peng Y, Gao Y, Gao H, Zhang J, Lv N, Miao Y and Lu Z: Insulin promotes invasion and migration of KRAS<sup>G12D</sup> mutant HPNE cells by upregulating MMP-2 gelatinolytic activity via ERK- and PI3K-dependent signalling. *Cell Prolif* 52: e12575, 2019.
28. Zhu W, Wu X, Yang B, Yao X, Cui X, Xu P and Chen X: miR-188-5p regulates proliferation and invasion via PI3K/Akt/MMP-2/9 signaling in keloids. *Acta Biochim Biophys Sin (Shanghai)* 51: 185-196, 2019.
29. Zong L, Wei X, Gou W, Huang P and Lv Y: Zinc improves learning and memory abilities of fetal growth restriction rats and promotes trophoblast cell invasion and migration via enhancing STAT3-MMP-2/9 axis activity. *Oncotarget* 8: 115190-115201, 2017.
30. Zhang W, Yin L, Song G, Han X, Yin Z and Luo D: LKB1 loss cooperating with BRAF V600E promotes melanoma cell invasion and migration by up-regulation MMP-2 via PI3K/Akt/mTOR pathway. *Oncotarget* 8: 113847-113857, 2017.
31. Beales ILP, Garcia-Morales C, Ogunwobi OO and Mutungi G: Adiponectin inhibits leptin-induced oncogenic signalling in oesophageal cancer cells by activation of PTP1B. *Mol Cell Endocrinol* 382: 150-158, 2014.
32. Allott EH, Lysaght J, Cathcart MC, Donohoe CL, Cummins R, McGarrigle SA, Kay E, Reynolds JV and Pidgeon GP: MMP9 expression in oesophageal adenocarcinoma is upregulated with visceral obesity and is associated with poor tumour differentiation. *Mol Carcinog* 52: 144-154, 2013.
33. Gonzales AJ, Goldsworthy TL and Fox TR: Chemical transformation of mouse liver cells results in altered cyclin D-CDK protein complexes. *Carcinogenesis* 19: 1093-1102, 1998.
34. Kokkinakis DM, Liu X and Neuner RD: Modulation of cell cycle and gene expression in pancreatic tumor cell lines by methionine deprivation (methionine stress): Implications to the therapy of pancreatic adenocarcinoma. *Mol Cancer Ther* 4: 1338-1348, 2005.
35. Chan KC, Wang CJ, Ho HH, Chen HM and Huang CN: Simvastatin inhibits cell cycle progression in glucose-stimulated proliferation of sortic vascular smooth cells by up-regulating cyclin dependent kinase inhibitors and p53. *Pharmacol Res* 58: 247-256, 2008.



This work is licensed under a Creative Commons Attribution-NonCommercial-NoDerivatives 4.0 International (CC BY-NC-ND 4.0) License.

RETRACTED